Revisiting thermal conductivity and interface conductance at the nanoscale

Brice Davier, Philippe Dollfus, N D Le, Sebastian Volz, J Shiomi, J Saint-Martin

Revisiting thermal conductivity and interface conductance at the nanoscale

B. Davier[1,2], P. Dollfus[1], N. D. Le[1], S. Volz[3], J. Shiomi[2], J. Saint-Martin[1]

[1] Université Paris-Saclay, CNRS, Centre de Nanosciences et de Nanotechnologies, 91120, Palaiseau, France

[2] Department of Mechanical Engineering, The University of Tokyo, Tokyo 113-856, Japan

[3] LIMMS UMI 2820, The University of Tokyo-CNRS, 4-6-1 Komaba, Meguro-ku, Tokyo 153-8505, Japan

Abstract

A simple and easy-to-handle semi-analytical model able to describe heat transport in heterostructures of length varying from the nano to the microscale is presented. It consists in redefining three intrinsic parameters: the ballistic thermal conductance, the effective thermal conductivity, and the interface thermal conductance by using two temperatures T^+ and T^- distinguishing the phonon populations according to the direction of their velocities instead of the standard pseudo-temperature *T*. The resulting model agrees well with the thermal conductance and temperature profiles predicted by advanced Monte Carlo simulation in all phonon transport regimes, i.e. diffusive, ballistic, and quasi-ballistic regimes, even in the presence of multiple interfaces. It is able to provide new insights into the interpretation of thermal properties of complex nanostructures.

I Introduction

The standard formalism of heat transport in solids, built in the nineteenth century by Fourier [1], is essentially based on two material properties: the heat capacity and the thermal conductivity. Using quantum mechanics and kinetic theory for phonons, the particle-like counterpart of lattice vibrations, Peierls established in 1929 [2] the heat theory that is still in use nowadays. By using this complex theoretical framework, the heat transport parameters can be computed numerically via ab-initio approaches generally based on Density Functional Theory (DFT) [3–7] and are now in a remarkable agreement with experimental data [8]. In bulk materials, spatial dimensions are, by definition, much longer than the mean free path of phonons, and the diffusive heat transport regime that takes place is perfectly captured by Fourier's formalism. In such systems, the energy distributions of phonons remain close to their equilibrium state according to the Bose-Einstein statistics.

These criteria are no longer valid in many recent devices based on nanostructures [9]. For instance, modern transistors are nanometer-long [10], and materials of interest in thermoelectrics are nanostructured, such as superlattices [11] or stacks of 2D materials [12,13]. In these systems, the size of which are of the same order of magnitude as or even smaller than the phonon mean free path, the phonon transport is out of equilibrium since the rate of scattering events encountered by phonons is not sufficient to let them recover their equilibrium distribution. Hence, more advanced heat transport formalisms must be considered, requiring generally the use of complex numerical simulations.

Most common numerical approaches are based on Molecular Dynamics [14,15] that calculates the classical trajectories of atoms. This powerful atomistic method is nevertheless limited by the size of the studied systems that is typically a few tens of thousands of atoms. Within the concept of phonon particles, other usual semi-classical approaches consider the Boltzmann transport equation for phonons (pBTE). This non atomistic formalism considers the phonon dispersion and scattering rates as input parameter and can more easily be used to investigate systems of various sizes from the nano- to the micro-scale. The particle Monte Carlo technique for solving stochastically the pBTE is particularly efficient and does not require any a priori assumption on the shape of the phonon distribution function [16–19]. Other approaches based on the Landauer formalism such as the Green's functions method [20,21] can deal with wave effects. However, a simple analytical modeling of heat transfer based on a set of a few parameters relevant at the nanometer scale remains highly desirable for practical use.

Accordingly, on the basis of different levels of approximations, several analytical models have been derived in order to model the heat flux and the effective conductivity in non-diffusive regimes. Starting from the Boltzmann's

transport equation and after simplifications of the distribution function, "Enhanced Fourier" laws were derived. They are based either on truncations of Fourier decompositions [23] [24], on Knudsen number expansion [25] or on spherical harmonic expansion [26] [22]. In Chen's Ballistic-Diffusive Equations [27] the heat flux is separated in its ballistic and diffusive contributions, while Regner et al. [28] and also Yang and Dames [29] have distinguished the heat fluxes propagating in forward and reverse directions. Likewise, Maassen and Lundstrom [30] have used the local temperatures associated with these oriented thermal fluxes.

Besides, much attention has been given to the investigation of heat transport across interfaces since the pioneering works of Kapitza [31]. To study the specific case of solid-solid interfaces, Little [32] adapted the Acoustic Mismatch Model (AMM) and later Swartz [33] developed the Diffusive Mismatch Model (DMM). Even if their underlying assumptions seem very different, these two models are based on a Landauer approach that considers the transmission of phonons emitted by ideal thermostats. However, though effective for many problems, they both lead to the so called virtual interface paradox as they predict a non-zero interface thermal resistance (or a finite conductance) in the case of an imaginary fully transparent interface (with a transmission of 1) located inside any homogeneous material [33]. Nevertheless, when considering the standard macroscopic model of resistances in series, we should be allowed to add any number of virtual interfaces within a structure, without increasing its total thermal resistance.

To overcome this paradox, the contribution of out of equilibrium phonons has been included by Simons [34], Chen [35] or Merabia et al. [36] for instance. From a solution of the Boltzmann transport equation in the linear regime (close to equilibrium), they derived a corrective term to modify the usual pseudo temperatures at the interface. However, these modified temperatures are generally phonon-mode-dependent [37], leading to models difficult to handle and even unable to correctly capture the fully ballistic transport regime. Maassen and Askarpour [38] used the forward and reverse heat fluxes and their related temperatures to simplify this problem. The most relevant temperature difference to consider at a thermal interface remains a current issue [39].

Revisiting the flux framework developed in Refs [40] and [38], the present work aims at introducing a simple heat transport model based on alternative definitions of effective thermal conductivity, interface thermal conductance and ballistic conductance by using two effective (not phonon-mode-dependent) pseudo temperatures distinguishing the populations of phonons according to the (positive or negative) direction of their velocity instead of the standard pseudo-temperature. Our approach generalizes the common macroscopic parameters of the Fourier formalism and extends their validity at the nanoscale (i.e. in the intermediate and ballistic transport regimes), in both homogeneous and inhomogeneous systems at steady state. The proposed analytical model is benchmarked against advanced Monte Carlo simulations for phonons using full-band 3D models of silicon phonon dispersion and phonon-phonon scattering rates [19].

II Homogeneous systems

To begin with, we only consider homogeneous structures, the temperature of which is set on both sides by thermostats. Without loss of generality, the hot thermostat is supposed to be on the left end while the cold one is on the right end, generating a heat transport in the positive direction of the *x* axis.

II.1. Thermal conductivity in diffusive regime

Within the framework of Fourier's law, the thermal conductivity $\kappa_{\text{diffusive}}$ in the diffusive regime (i.e. in a system much longer than the phonon mean free path) is the proportionality factor between the heat flux density Q and the local temperature gradient along the transport direction x, i.e.

$$Q = -\kappa_{\text{diffusive}} \frac{\partial T}{\partial x} \tag{1}$$

According to Peierls' model the bulk thermal conductivity of a material is expressed as [36]

$$\kappa = \frac{\Omega}{(2\pi)^3} \sum_s \hbar\omega_s \left|v_{s,x}\right| l_s \frac{\partial f_{\text{BE}}}{\partial T}(\omega_s, \bar{T}) \tag{2}$$

where $\bar{T}$ refers to the average temperature in the system, and l_s to the mean free path parameter for a phonon in state s. The quantities ω_s and v_s are the angular frequency and velocity in the state *s*, respectively, while Ω is the volume of the considered reciprocal space and f_{BE} is the Bose-Einstein distribution. The summation on the reciprocal states is made over all states *s* of the Brillouin zone.

In the diffusive regime, a local model of l_s based only on the properties of the material is sufficient, i.e.,

$$l_{s,\mathrm{diffusive}} = \frac{|v_{s,x}|}{\lambda_s}$$

where λ_s is the total scattering rate for a phonon in state s within the relaxation time approximation. The diffusive, i.e. bulk, conductivity is thus

$$\kappa_{\mathrm{diffusive}} = \frac{\Omega}{(2\pi)^3}\sum_s \hbar\omega_s \frac{|v_{s,x}|^2}{\lambda_s}\frac{\partial f_{\mathrm{BE}}}{\partial T}(\omega_s, \bar{T}) \tag{3}$$

However, in non-diffusive regime, this formula is no longer representative of the actual heat transport since the effective mean free path is affected by the size of the structure. This is particularly true in a fully ballistic system in which the temperature gradient in Eq. 1 vanishes.

II.2. Thermal conductance in ballistic regime

In short systems working in ballistic transport regime, i.e. in the absence of phonon scattering, the total thermal flux density Q through the device is directly given by the difference of thermal flux densities Q_{hot} and Q_{cold} emitted from the external thermostats at temperatures T_{hot} and T_{cold}, respectively. Each of the two phonon populations injected in the system, i.e. having a positive or negative velocity for Q_{hot} or Q_{cold}, respectively, occupies only one half of the total phonon states. Thus, using the Landauer's formalism with a transmission equal to unity, Q can be written as

$$Q = Q_{\mathrm{hot}} - Q_{\mathrm{cold}} = \frac{\Omega}{(2\pi)^3}\left[\sum_{\substack{s \\ v_{s,x}>0}} \hbar\omega_s |v_{s,x}| f_{\mathrm{BE}}(\omega_s, T_{\mathrm{hot}}) - \sum_{\substack{s \\ v_{s,x}<0}} \hbar\omega_s |v_{s,x}| f_{\mathrm{BE}}(\omega_s, T_{\mathrm{cold}})\right]$$

$$Q = \frac{1}{2}\frac{\Omega}{(2\pi)^3}\sum_s \hbar\omega_s |v_{s,x}|\left(f_{\mathrm{BE}}(\omega_s, T_{\mathrm{hot}}) - f_{\mathrm{BE}}(\omega_s, T_{\mathrm{cold}})\right) \tag{4}$$

For a small temperature difference $\Delta T_{\mathrm{contacts}} = T_{\mathrm{hot}} - T_{\mathrm{cold}}$, the first order gradient expansion gives

$$f_{\mathrm{BE}}(\omega_s, T_{\mathrm{hot}}) - f_{BE}(\omega_s, T_{\mathrm{cold}}) \approx \frac{\partial f_{\mathrm{BE}}}{\partial T}\Delta T_{\mathrm{contacts}}$$

Then, the heat flux density may be rewritten by defining a ballistic thermal conductance $G_{\mathrm{ballistic}}$ as

$$Q = \left(\frac{1}{2}\frac{\Omega}{(2\pi)^3}\sum_s \hbar\omega_s |v_{s,x}|\frac{\partial f_{\mathrm{BE}}}{\partial T}\right)\Delta T_{\mathrm{contacts}} = G_{\mathrm{ballistic}}\,\Delta T_{\mathrm{contacts}} \tag{5}$$

It is worth noting that in a ballistic system [41,42], the conductance is size independent, but depends only on the phonon dispersion.

II.3. Hemispherical temperatures

The concept of temperature, strongly related to the equilibrium Bose-Einstein statistics of phonons, is ill-defined in non-diffusive heat transport regimes because the distribution of phonons may be far from equilibrium. It is however still convenient to propose another definition of the temperature since this quantity is mandatory in the widely used previous equations. Usually, a pseudo temperature T is defined as the temperature leading to the same phonon energy density as the actual energy density [19], but using an equilibrium distribution of phonons at this temperature T. This definition matches the standard definition of the temperature in systems at equilibrium but naturally extends it in system where strong out of equilibrium conditions occur.

To properly define the effective conductivity or to treat the case of heat transport through interfaces, we have to separate the phonon distribution in two parts: one related to the "forward" phonons having a positive velocity component along the direction of the main heat flux, and another related to the remaining "backward" phonons having a negative velocity [30].

Like other pseudo temperatures relevant under equilibrium as well as out of equilibrium conditions, the "hemispherical" temperatures T^+ and T^- are defined from the actual energy density, but only from the density related to the phonon population with positive and negative velocity, respectively. Finally, T^+ and T^- are defined as the parameters satisfying the following relationship:

$$E^{+/-}\left(T^{+/-}\right) = \frac{\Omega}{(2\pi)^3} \sum_{\substack{s \\ v_s>0 \,/\, v_s<0}} \hbar\omega_s f_{\mathrm{BE}}(\omega_s, T^{+/-}) \tag{6}$$

where $E^{+/-}$ stands for the actual energy density of the forward/backward phonons. At equilibrium all the previous pseudo temperatures are equal ($T^+ = T^- = T$) and correspond to the usual temperature definition.

In the present work, the use of this pseudo temperature T is systematically replaced by the use of hemispherical temperatures T^+ and T^-. In what follows, two distinct temperature differences are used for any homogeneous section. The first one, called $\Delta T_{\mathrm{contacts}}$, is the difference of temperature between incoming phonons onto this section (i.e. between phonons at the left boundary with a positive velocity and phonons at the right boundary with a negative velocity). For a section of length L, we thus have: $\Delta T_{\mathrm{contacts}} = T^+(x = 0) - T^-(x = L)$. It should be emphasized that in the case of perfect thermostats, i.e. that act as perfect black-body emitters (and also as ideal absorbers), $\Delta T_{\mathrm{contacts}}$ is directly the temperature difference of the thermostats but differs from the common pseudo-temperature difference $T(x = 0) - T(x = L)$. Thus, the hemispherical temperatures are easier to manage experimentally than the pseudo temperature T even if it seems counter-intuitive.

The second temperature difference is a local one called $\Delta T_{\mathrm{local}}$ defined at any position x as the difference between the hemispherical temperatures: $\Delta T_{\mathrm{local}}(x) = T^+(x) - T^-(x)$.

II.4. Effective thermal conductivity

To bridge the gap between diffusive and ballistic heat transport regimes, we propose to use an effective thermal conductivity $\kappa_{\mathrm{effective}}$ (called apparent conductivity in [40]) that is not defined from the temperature gradient but by using the hemispherical temperature difference between the incoming phonons on each sides of the section, i.e. the temperature difference $\Delta T_{\mathrm{contacts}}$ as defined above. In a system of length L between the thermostats, we thus define $\kappa_{\mathrm{effective}}$ as

$$Q = \kappa_{\mathrm{effective}} \frac{\Delta T_{\mathrm{contacts}}}{L} \tag{7}$$

By using this definition, $\kappa_{\mathrm{effective}}$ and $\kappa_{\mathrm{diffusive}}$ (see Eq. 1) are equivalent in the diffusive regime, i.e. in systems much longer than the mean free path of phonons.

In a ballistic system where the temperature gradient vanishes, a ballistic thermal conductivity $\kappa_{\mathrm{ballistic}}$ cannot be defined from the usual definition of Eq. 1. However, combining Eq. 5 and Eq. 7 gives

$$\kappa_{\mathrm{ballistic}} = \frac{\Omega}{(2\pi)^3} \sum_s \hbar\omega_s \left|v_{s,x}\right| \frac{L}{2} \frac{\partial f_{\mathrm{BE}}}{\partial T}(\omega_s, \bar{T}) = L\, G_{\mathrm{ballistic}} \tag{8}$$

Interestingly, performing a term-to-term identification of the mean free path between Eq. 8 obtained by using a Landauer's formalism and Eq. 2 obtained by using a Boltzmann's formalism, we obtain $l_{s,\mathrm{ballistic}} = \frac{L}{2}$. Indeed, in ballistic regime, the mean free path only depends on the device length. The ballistic thermal conductivity is thus proportional to the distance between the thermostats L. The factor of $\frac{1}{2}$ comes from that in the ballistic conductivity $G_{ballistic}$ calculated within the Landauer's formalism only one half of phonon states are considered (see [43]). A physical interpretation of this mathematical result $l_{s,\mathrm{ballistic}} = \frac{L}{2}$ is that the average distance the phonons (uniformly distributed in the device) have to cover along the transport direction before colliding with a thermostat is actually $\frac{L}{2}$, not L.

The simplest approach to the effective thermal conductivity in the intermediate transport regime, i.e. between the diffusive and the ballistic ones, depending on both the material properties and the structure, is provided by the following non-spectral Matthiessen rule

$$\frac{1}{\kappa_{\text{effective,non-spectral}}} = \frac{1}{\kappa_{\text{ballistic}}} + \frac{1}{\kappa_{\text{diffusive}}} \tag{9}$$

To get a more accurate estimation of the effective conductivity, a spectral Matthiessen summation for the mean free path must be applied. Additionally, the spectral mean free path should also depend on the device geometry. For instance, for a single homogeneous system (i.e. a nanofilm in cross-plane configuration), the spectral mean free path of state s writes [19]

$$\frac{1}{l_{s,\text{spectral}}} = \frac{1}{l_{s,\text{ballistic}}} + \frac{1}{l_{s,\text{diffusive}}} = \frac{\lambda_s + 2\frac{|v_{s,x}|}{L}}{|v_{s,x}|} \tag{10}$$

Different effective thermal conductivities (defined in Eq. 2) are plotted in Figure 1 for silicon nanofilms in cross plane configuration, as a function of their length L. The non-spectral (cf. Eq. 9) and spectral (cf. Eq. 10) effective thermal conductivities are compared to the results of Monte Carlo simulation (MC) using directly Eq. 7. The MC simulator used here has been detailed in [19]. As expected, all models converge asymptotically to the ballistic and diffusive limits. However, the predictions of the simple non-spectral Matthiessen approximation (Eq.9) differ from the MC results in the intermediate regime, up to 60% at $L = 200\text{nm}$. The spectral model results (Eq. 10, solid blue line) agree with the MC ones in the full range of L [44] with a relative error lower than 1%. Hence, in a homogeneous system, considering the spectral evolution of the mean free path provides a significant improvement of the quantitative prediction of k_{eff} in the intermediate transport regime.

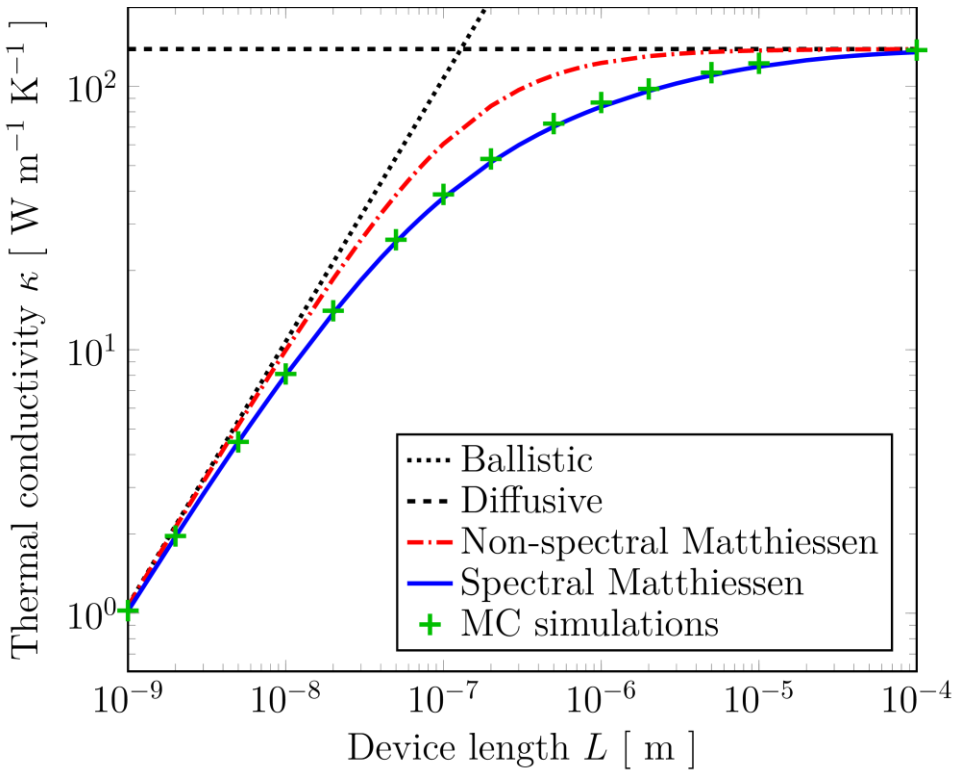

Figure 1: Thermal conductivities of silicon nanofilms in cross-plane configuration as a function of the device length predicted from: the ballistic model (short dashed line, Eq. 8), the diffusive model (long dashed line, Eq. 3), Monte Carlo (MC) simulations (green crosses), the non-spectral Matthiessen approximation (red dashed line, Eq. 9), the spectral Matthiessen approximation (blue line, Eq. 10). T=300 K.

II.5. Central relationships

At any point x, by using the local hemispherical temperatures T^+ and T^- defined above, the heat flux density can be separated into its forward and backward parts, leading to

$$Q = Q|_{v_x>0} - Q|_{v_x<0} = \frac{1}{2}\frac{\Omega}{(2\pi)^3}\sum_s \hbar\omega_s|v_{s,x}|\left(f_{BE}(\omega_s, T^+(x)) - f_{BE}(\omega_s, T^-(x))\right) \quad (11)$$

For a small temperature difference $\Delta T_{\text{local}}(x)$, the first order gradient expansion gives

$$f_{BE}(\omega_s, T^+) - f_{BE}(\omega_w, T^-) \approx \frac{\partial f_{BE}}{\partial T}(T^+ - T^-) = \frac{\partial f_{BE}}{\partial T}\Delta T_{\text{local}}(x)$$

The heat flux density in Eq. 11 can thus be rewritten as (see also [45]):

$$Q = \frac{1}{2}\frac{\Omega}{(2\pi)^3}\sum_s \hbar\omega_s|v_s|\frac{\partial f_{BE}}{\partial T}\Delta T_{\text{local}}(x) = G_{\text{ballistic}}\,\Delta T_{\text{local}} \quad (12)$$

This formula is remarkable in the sense that for any homogeneous system, regardless of the transport regime, the heat flux density is written as the product of the ballistic thermal conductance of the material (defined in Eq. 5 and only requiring the prior knowledge of the phonon dispersion) and the local difference of hemispherical temperatures [30]. Hence, in steady-state regime, ΔT_{local} is uniform (except at interfaces, as investigated in what follows).

By applying the conservation of the heat flux to combine Eq. 7 and Eq. 12, we obtain the second central relationship between the local and contact temperature differences as

$$\Delta T_{\text{local}} = \Delta T_{\text{contacts}}\frac{\kappa_{\text{effective}}}{L\ G_{\text{ballistic}}} \quad (13)$$

Hence, in the case of a diffusive transport regime in which the phonon distribution remains close to equilibrium, we have $\kappa_{\text{effective}} \approx \kappa_{\text{diffusive}} \ll \kappa_{\text{ballistic}} = L\ G_{\text{ballistic}}$, leading to $\Delta T_{\text{local}} = 0$ and $T^+ = T^- = T$. At equilibrium, all pseudo temperature definitions converge to the standard one. In the opposite case that is the ballistic transport regime, $\kappa_{\text{effective}} \approx \kappa_{\text{ballistic}} = L\ G_{\text{ballistic}}$ and thus $\Delta T_{\text{local}} = \Delta T_{\text{contacts}}$, i.e. the temperature gradients vanish: for any position x, $T^+(x) = T^+(0)$ and $T^-(x) = T^-(L)$.

It must be emphasized that Eq. 12 and its consequences, for instance on, Eq. 13, are the key points of the present work. Indeed, its outcomes are relevant not only in the case of a homogeneous system but especially in the case of heterostructures as it is discussed in the next section.

III Heterogeneous systems

More complex structures such as junctions and superlattices can be studied by introducing a model of solid-solid interface.

III.1. Interface thermal conductance based on hemispherical temperatures

At each interface between two materials, a thermal boundary conductance G^I is expressed as

$$Q = G^I\,\Delta T^I_{\text{std}} \quad (14)$$

where ΔT^I_{std} is the temperature drop at the interface. As discussed in the previous section, the proper definition of temperature to be used here is a crucial issue [35].

The common procedure uses the standard pseudo temperature, which is calculated from the full distribution of phonons on each side of the interface located at a given position x^I as follows

$$\Delta T^I_{\text{std}} = T(x^I - \delta x) - T(x^I + \delta x) \quad (15)$$

When using this equation, the choice of the value of δx may be an issue. For instance, in Ref. [36] the phonon mean free path is used to defined δx but it is complex to implement, due in particular to the fact that the mean free path has a significant spectral dependence.

However, the use of hemispherical temperatures is more consistent with the initial definition of the interface thermal conductance from [33], since it only includes the phonons that actually interact with the interface. Thus, we propose in this work an original definition of the thermal boundary conductance G^I using T^+ and T^- to define the temperature drop at interface. It yields:

$$G^I = \frac{Q}{\Delta T^I_{\text{local}}}$$

with $$\Delta T^I_{\text{local}} = T^+(x^I - \epsilon) - T^-(x^I + \epsilon) \quad (16)$$

where ϵ is an infinitely short distance.

One advantages of the formulation based on $\Delta T^I_{\text{local}}$ for extracting the interface conductance is that it naturally models virtual interfaces (without requiring new variable ingredient such as the value of δx in Eq. 15). Another important advantage is that for a transparent interface, i.e. having a transmission equal to unity, located anywhere inside a material, we have $\Delta T^I_{\text{local}} = \Delta T_{\text{local}} = T^+ - T^-$ and the related interface thermal conductance is $G^I = G_{\text{ballistic}}$ (cf. Eq 12) that corresponds to the maximum value of conductance. In contrast, the paradox corrected formulation of G^I based on ΔT^I_{std}, yields a temperature difference of 0 K at a transparent interface since the standard pseudo-temperature must be continuous in a homogeneous system. Thus, an (unphysical) infinite conductance (better than in the ballistic case), i.e. a zero resistance, is obtained. Finally, the use of ΔT^I_{std}leads to another (weak) virtual interface paradox as a virtual interface is expected to be ballistic.

III.2. Interface modeling: Simple case of homojunction

To compare the two previous definitions of G^I, homojunctions made of two identical silicon films of various lengths separated by a rough, i.e. fully diffusive, interface have been investigated. The transmission coefficient of each phonon colliding with this diffusive interface t_s is ½ according to the Diffusive Mismatch Model [33]. It should be mentioned that the type of interface modeling (here DMM) is not a key point here as in this simple system (diffusive homojunction), the value of 0.5 for the transmission is standard in almost all approaches. Besides, in all our MC simulations (here and in the following parts) the thermostats are modeled as perfect black-body emitters and also as ideal absorbers, i.e. all phonons with the relevant velocity (e.g. with a positive velocity for phonon in the left thermostat) are emitted from the thermostat and injected in the device while phonons in contact reaching a boundary with the a thermostat disappear from the simulation. Thus, no size effect is expected due to influence of the thermostats, as shown in Ref [46].

By using this transmission coefficient, this interface has been implemented in our Monte Carlo simulator for phonons [19] from which we can straightforwardly calculate the temperatures T, T^+ and T^- (whatever the transport regime), the flux and thus the different forms of the interface thermal conductance according to their definition.

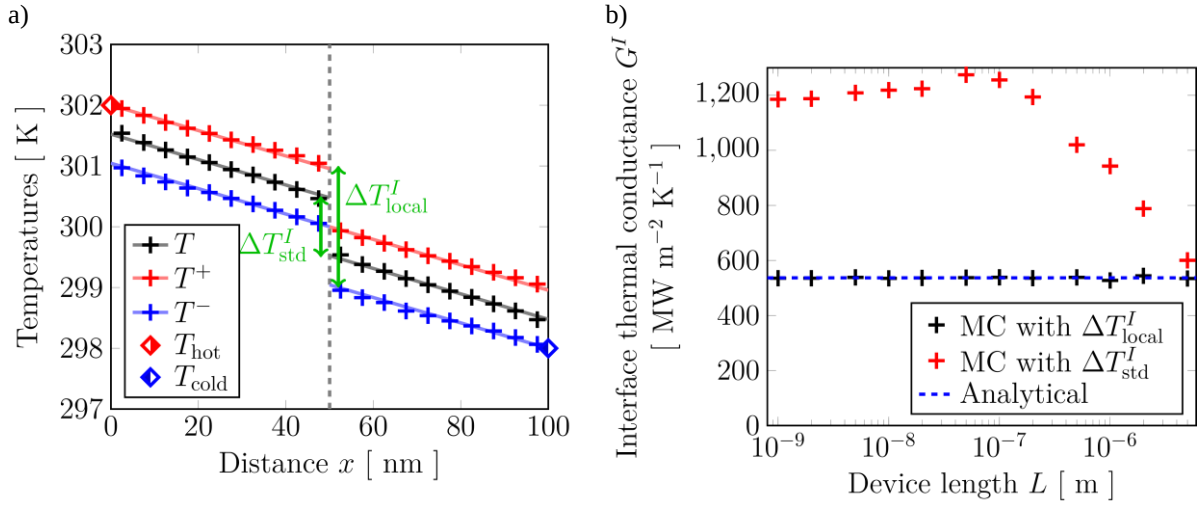

Figure 2: In diffusive Si/Si junctions: a) temperature profiles T (black), T^+ (red) and T^- (blue) for a system of length $L = 100$nm calculated by a Monte Carlo simulation, b) interface thermal conductance as a function of the device length, calculated from the analytical formula (blue dashed line) and Monte Carlo (MC) results using Eq. 15 i.e. ΔT^I_{std} (red crosses) and Eq. 16 i.e. $\Delta T^I_{\text{local}} = T^+ - T^-$ (black crosses)

Figure 2.a) shows the temperature profiles of the pseudo temperature T (black), and the hemispherical temperatures T^+ (red) and T^- (blue) along the transport direction x in a junction of length $L = 100$ nm. The thermostat temperatures are $T_{\text{hot}} = 302$ K and $T_{\text{cold}} = 298$ K.

At each contact, a temperature jump of the pseudo-temperature T is clearly visible in the MC results. In contrast the hemispherical temperatures T^+ and T^- are continuous (no jump) near the hot and cold thermostats, respectively. However, the temperature jumps of T^- and T^+ near the hot and cold thermostats, respectively, are higher than for T. It should be emphasized that, as the heat flux is uniform and in accordance with Eq. 12, the difference between the two local hemispherical temperatures ΔT_{local} in each part of the junction is also uniform.
The temperature differences at the interface are different, as $\Delta T^I_{\mathrm{std}}$ = 1 K (using the shortest available δx in Eq. 15) is two times smaller than $\Delta T^I_{\mathrm{local}}$ = 2 K. These two quantities lead to the different interface thermal conductances plotted in Figure 2.b). The interface thermal conductances obtained by using $\Delta T^I_{\mathrm{std}}$ and $\Delta T^I_{\mathrm{local}}$, respectively, are plotted in red and black crosses, respectively. For comparison, the results provided by the standard analytical formula that can be found in Ref. [46], considered as a reference in this simple case, are indicated by a blue dashed line. Remarkably, the results obtained from the use of the $\Delta T^I_{\mathrm{local}}$ temperature difference reproduce the analytical DMM results for all device lengths. In contrast, the use of $\Delta T^I_{\mathrm{std}}$ (red crosses) leads to values up to two times higher than the analytical results in short devices and gives rise to an unexpected length-dependence in long devices. Similar results have been obtained in [39].

Using the parameters defined above, considering only $\Delta T_{\mathrm{local}}$ and $\Delta T_{\mathrm{contact}}$ and thus adopting a Landauer point of view, a comprehensive and easily tractable analytical model of thermal transport in heterostructures is presented in the next section.

III.3. Analytical model of thermal transport in heterostructures

Typical profiles of temperatures T, T^+ and T^- in a heterojunction are plotted in Figure 3. The temperature differences introduced in the previous section, $\Delta T_{\mathrm{contact}}$ and $\Delta T_{\mathrm{local}}$, are defined on both halves of the structure, and distinguished by superscript L (resp. R) for the left (resp. right) part. Notably, $\Delta T^L_{\mathrm{contact}}$ is now the difference between the temperature of the hot thermostat and the temperature of right-coming phonons from the left side of the interface, while $\Delta T^R_{\mathrm{contact}}$ is the difference between the temperature of left-coming phonons from the right side of the interface and the temperature of the cold thermostat. The temperature drop at the interface is $\Delta T^I = \Delta T^I_{\mathrm{local}}$.

Then, the total temperature difference between the left thermostat at a temperature T_{hot} and the right thermostat at a temperature T_{cold} can be decomposed as

$$T_{\mathrm{hot}} - T_{\mathrm{cold}} = \Delta T^L_{\mathrm{contact}} - \Delta T^L_{\mathrm{local}} + \Delta T^I_{local} \quad - \Delta T^R_{\mathrm{local}} + \Delta T^R_{\mathrm{contact}} \tag{18}$$

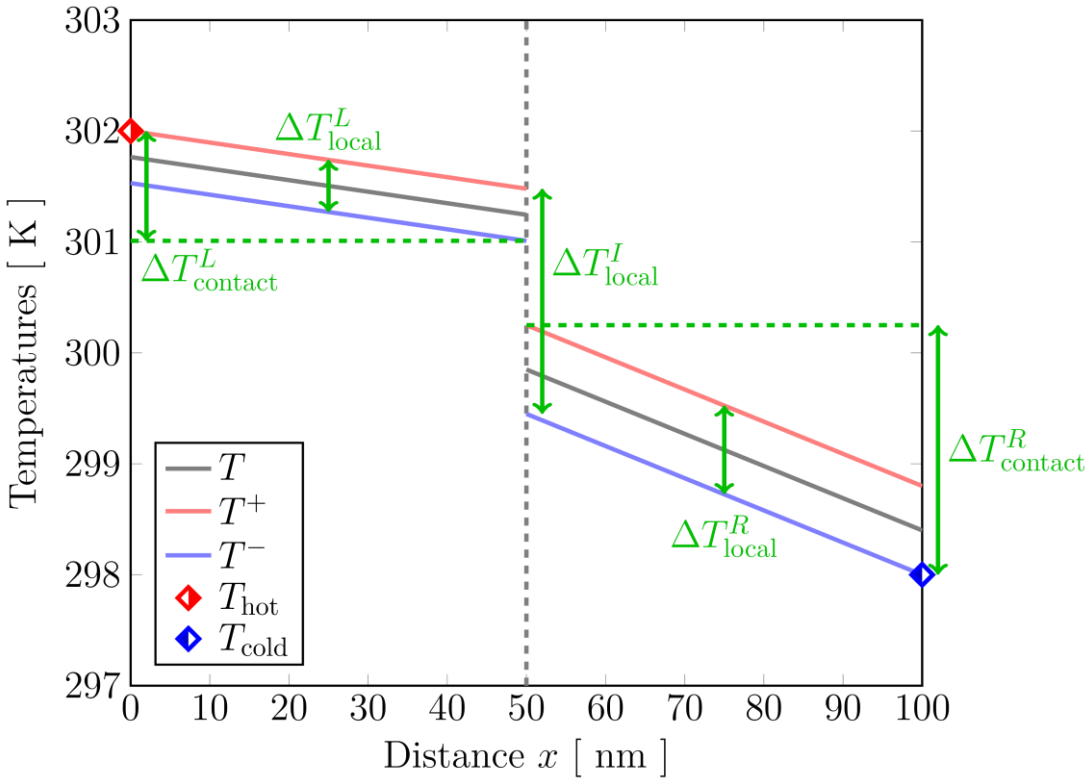

Figure 3: Typical profiles of the average temperature T (black), and the hemispherical temperatures T^+ (red) and T^- (blue) in a heterojunction. Diamonds show the temperature of the hot (red) and cold (blue) thermostats. $\Delta T^L_{\text{contact}}$ and $\Delta T^R_{\text{contact}}$ are the temperature differences between the phonons incoming respectively in the left and right part. $\Delta T^L_{\text{local}}$ and $\Delta T^R_{\text{local}}$ are the temperature differences between the hemispherical temperatures, respectively in the left and right part. ΔT^I is the difference between hemispherical temperatures across the interface.

Since the thermal flux is conserved throughout the structure, using the Eqs. 12, 13 and 14 we obtain

$$Q = \frac{\kappa^{L/R}_{\text{effective}}}{L^{L/R}} \Delta T^{L/R}_{\text{contact}} = G^I . \Delta T^I = G^{L/R}_{\text{ballistic}} . \Delta T^{L/R}_{\text{local}} \tag{19}$$

Finally, the total conductance of the heterojunction G^{total} is expressed as a function of the interface conductance G^I, the effective conductivities of the involved materials and also their ballistic conductance, i.e.

$$G^{\text{total}} = \frac{Q}{T_{\text{hot}} - T_{\text{cold}}} = \left[\frac{L^L}{\kappa^L_{\text{effective}}} - \frac{1}{G^L_{\text{ballistic}}} + \frac{1}{G^I} - \frac{1}{G^R_{\text{ballistic}}} + \frac{L^R}{\kappa^R_{\text{effective}}} \right]^{-1} \tag{20}$$

The previous model must be compared to the basic model of the three resistances in series, i.e. those of the left and right parts plus those of the interface, which gives

$$G^{\text{total}}_{\text{std}} = \left[\frac{L^L}{\kappa^L_{\text{diffusive}}} + \frac{1}{G^I} + \frac{L^R}{\kappa^R_{\text{diffusive}}} \right]^{-1} \tag{21}$$

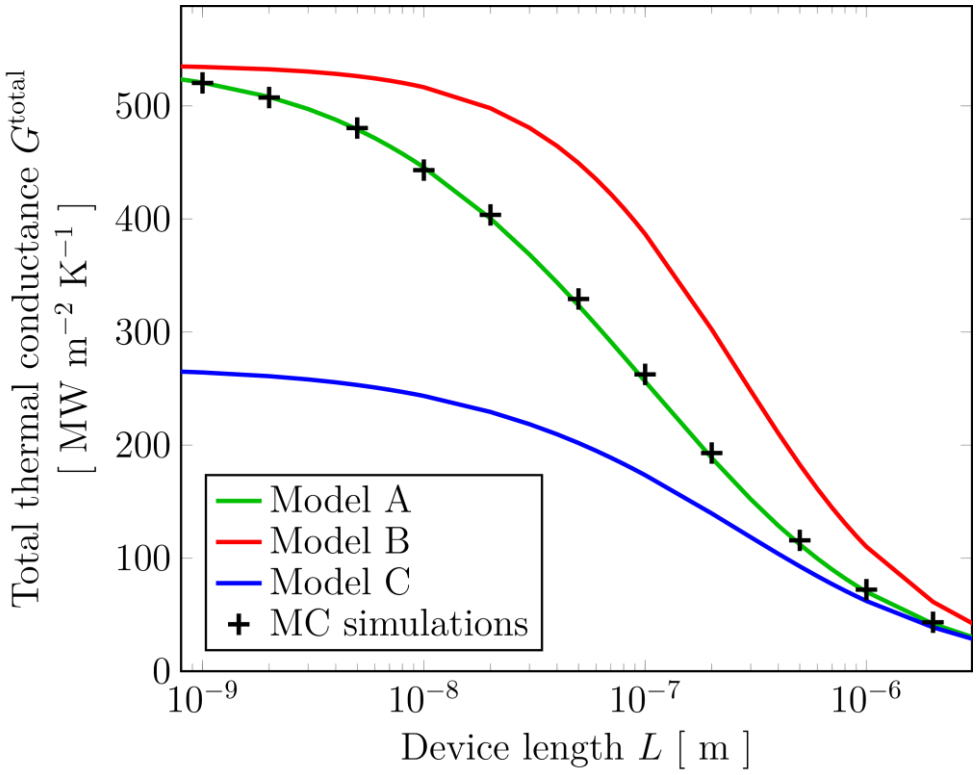

Figure 4: Total thermal conductance of diffusive Si/Si junctions versus length from MC simulations (crosses) and several analytical models (lines). Model A (green) is our proposed model in Eq. 20. Model B (red) is the standard model of resistances in series in Eq. 21. Model C (blue) is a modification of Model B, replacing the diffusive conductivities with the effective conductivities. T = 300 K.

In the case of the diffusive Si/Si homojunction (with temperature profiles shown in Figure 2), the total conductance provided by three analytical models is plotted in Figure 4 and compared with their numerical Monte Carlo counterpart. Model A (green line) is our new approach (cf. Eq. 20) including the semi-analytical effective conductivities from Eq. 10 (i.e. considering the spectral Mathiessen-like summation of the mean free path). Model B (red line) corresponds to the classical approach with three thermal resistances in series (see Eq. 21). Model C is the naïve model based on a modified version of Eq. 21 where the semi-analytical effective conductivities $\kappa^{L/R}_{\text{effective}}$ from Eq. 10 are used instead of the diffusive conductivities $\kappa^{L/R}_{\text{diffusive}}$.

Counterintuitively, model C is very disappointing as it strongly underestimates the conductance and cannot capture the ballistic regime. The use of effective thermal conductivities is not a sufficient ingredient to accurately describe the out-of-equilibrium regime. Model B is more satisfactory, except in the intermediate regime where it overestimates by over 50% the MC results. Model A, our proposed model, is in agreement with the MC simulation with errors less than 5% over the entire length range, i.e. in all transport regimes.

The semi-analytical approach of Eq. 21 can be extended in the case of multiple interfaces. Indeed, the total thermal conductance G^{total} in a heterostructure made of N homogeneous materials (of length L_i, with effective thermal conductivity $\kappa^{i}_{effective}$.) is obtained by mixing Eqs. 2 and 4. By noting $G_I^{i,i+1}$ the thermal conductance of the interface between materials *i* and materials *i+1*, we finally obtain:

$$G^{total} = \frac{Q}{T_{hot} - T_{hold}} = \frac{\kappa^{total}_{effective}}{\sum_i L_i} = \left[\sum_{i=1}^{N} \frac{L_i}{\kappa^{i}_{effective}} + \sum_{i=1}^{N-1} \left(-\frac{1}{G^{i}_{ballistic}} + \frac{1}{G_I^{i,i+1}} - \frac{1}{G^{i+1}_{ballistic}} \right) \right]^{-1} \qquad (22)$$

In this general expression, the difference with the common resistances in series approach is even more clear and due to the contribution of the ballistic conductance in each side of the interface.

As examples of systems with multiple interfaces, double Si/Ge heterojunctions (with two Si/Ge interfaces) are studied and compared to a simple Si/Ge heterostructures. In simple heterojunctions the Si/Ge interface is located

in the middle of the heterojunction (i.e. at $x = L/2$). In double heterojunctions the interfaces are at positions $x = L/3$ and $x = 2L/3$. Two sequences of materials are investigated, i.e. Si/Ge/Si and Ge/Si/Ge. In Figure 5, the total conductances for simple and double heterostructures of different lengths are plotted. The lines are related to analytical results computed by using Eq. 22 where the values of $\kappa_{effetive}$ and $G_{ballistic}$ in Si and Ge are obtained via Eq. 2 with mean free path of Eqs. 10 and 8, respectively, both requiring only the prior knowledge of the phonon dispersion and the diffusive mean free path in Ge and Si. Symbols are results provided by our MC simulation using DMM transmission coefficients [48]. The presented semi-analytical results remarkably reproduced the numerical results from the nano to microscale. The models A and C used in Figure 4 provide much less relevant results (not shown), in particular in the intermediate regime.

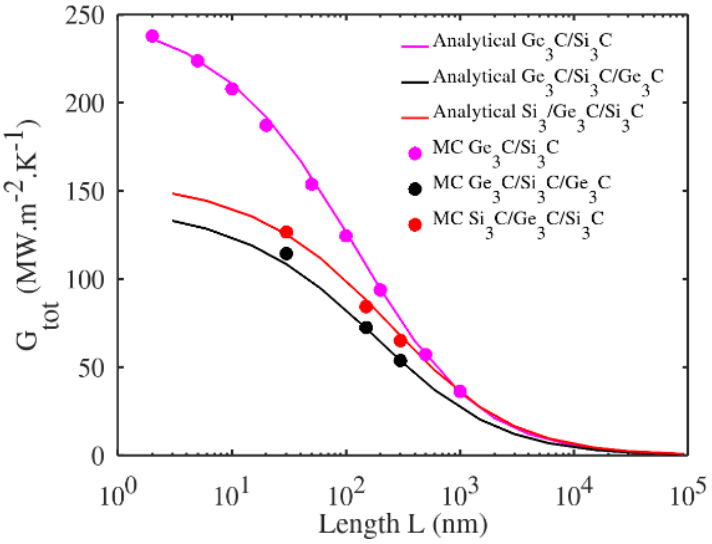

Figure 5: Total thermal conductance of the Si/Ge simple and double heterostructures: Monte Carlo results vs. semi-analytical model of Eq. 22. T = 300 K.

IV Discussion

The presented formalism is based on only three parameters: the effective conductivity $\kappa_{\text{effective}}$, the ballistic conductance $G_{\text{ballistic}}$ and the interface thermal conductance G^I. All these parameters are material dependent and $\kappa_{\text{effective}}$ is also geometry dependent. They can be computed semi-analytically from the phonon dispersion and the phonon scattering rates. The definition of these parameters is based on the two hemispherical temperatures T^+ and T^- that take the role of the pseudo temperature T in the standard heat transport model. It thus offers the advantage that the boundary temperatures of T^+ or T^- strictly match the temperature of the corresponding contact thermostat in all transport regimes. All the temperature jumps at internal interface as well at the boundaries are related to T^+ and T^-, instead of T in standard models. Moreover, each temperature jump is associated with the presence of $G_{ballistic}$ terms either in the equation of the effective conductivity $\kappa_{\text{effective}}$ (Eq. 23) or in the equation of the total conductance G_{total} (Eq. 22).

Our approach is not limited to the use of the DMM for the interface conductance G_{int}. By principle, any type of G_{int} estimate can be used as input in our approach. The full band version of the DMM is considered in this work because it is, to our knowledge, the most accurate method to semi-analytically calculate interface thermal conductances at room temperature.

In this article, all types of phonon transport regimes, from fully ballistic to diffusive, are studied. Both the temperature and the length of the device influence the nature of transport in the device. Since temperature also has an impact on the equilibrium distribution function and not just on the transport regime, we have chosen to focus first on the effect of the length of the device. The results presented were obtained around 300 K with a thermostat temperature bias of up to 10 K. However, as the parameters of our model are temperature dependent, a wide temperature range from ultra-low to very high temperatures remains to be investigated.

This model assumes that hemispherical phonon distributions stay close to equilibrium hemispherical distributions, so that the related temperatures are meaningful. This assumption is perfectly valid in the two extreme cases that are the diffusive and ballistic regimes. In the intermediate regime, our approach seems reasonable as it reproduces the Monte Carlo results that give the exact phonon distributions in the case of "semi-transparent" interfaces. Moreover, in the proposed analytical model, the use of these hemispherical temperatures appears straightforward and for instance more convenient than the ballistic and diffusive temperatures defined in Ref. 35 at each face of an interface. Nevertheless, it should be mentioned that the presented framework of a two-flux approach is strongly related to a 1D transport problem and its ability to be generalized to systems where 2D transport effects may occur remains an open issue.

The presented model naturally eliminates the virtual interface paradox thanks to the concept of ballistic thermal conductance. However, as early as 1959, Little [32] defined the interface thermal conductance of a virtual interface, or any interface with perfect transmission, as equal to the thermal conductance of a mean-free-path-long section of the material. This was conceptually equivalent to the ballistic thermal conductance: in both cases, each phonon undergoes one single phonon-phonon scattering event.

In addition, we would like to emphasize that in the case of a constant temperature gradient ∇T in a homogeneous structure, a parameter $\kappa_{\text{effective},\nabla\text{T}}$ obtained by using the local temperature gradient ∇T can be defined and related to our effective thermal conductivity $\kappa_{\text{effective}}$ (defined in Eq. 9) as

$$\kappa_{\text{effective},\nabla\text{T}} = -\frac{Q}{\nabla\text{T}} = \left[\frac{1}{\kappa_{\text{effective}}} - \frac{1}{L.G_{\text{ballistic}}}\right]^{-1} \tag{23}$$

Apart from its divergence at the ballistic limit as the temperature gradient vanishes, $\kappa_{\text{effective},\nabla\text{T}}$ could be used to derive an expression equivalent to Eq. 20. However, a formalism based on $\kappa_{\text{effective},\nabla\text{T}}$ (i.e. on the local temperature gradient) is less appealing as a linear profile of temperatures is assumed, which may be relatively inaccurate in the intermediate regime as shown for instance in Fig 6.a of Ref [40], and a specific ballistic conductance term would have to be added at each contact, as done in Ref. [38].

Remarkably, introducing the non-spectral Matthiessen approximation for the effective conductivities, i.e. using $\kappa_{\text{effective}}$ in the approximation of Eq 9, in our model of the total conductance (Eq. 20) simply yields the formula obtained when considering three thermal resistances in series (i.e. Eq. 21). Indeed, the non-spectral approach for $\kappa_{\text{effective}}$ leads to annihilation (or perfect compensation) of the terms containing the ballistic conductance. Thus, a formula containing only the resistances of the left and right films (defined by using the standard diffusive thermal conductivity $\kappa_{\text{diffusive}}$ in Eqs. 1 and 2 instead of $\kappa_{\text{effective}}$) plus the interface resistance is recovered. Astonishingly, our model shows that the Fourier approach (just based on $\kappa_{\text{diffusive}}$) remains relevant in the case of heterostructure in all transport regimes. Improving the accuracy of the model in the intermediate transport regime requires the full spectral approach of $\kappa_{\text{effective}}$ as well as the addition of the ballistic conductance contributions in the thermal interface conductance.

Finally, we believe that our formalism, simple to handle, can be useful for the community as it clearly brings to light the role of the ballistic conductance and its contribution to heat transport in nanostructures. It also provides a very convenient set of parameters separating clearly the contributions of materials ($G_{ballistic}$, $\kappa_{\text{effective}}$), geometry ($\kappa_{\text{effective}}$) and interfaces ($G^I$). The definitions of effective thermal conductivity and interface conductance based on hemispherical temperatures can be easily used in many simulation frameworks of thermal transport such as Molecular Dynamics. In parallel, the experimental evaluations of these parameters in nanostructures could provide new insights into the heat transport at the nanoscale.

V Conclusion

A change of point of view in thermal modeling by redefining all the thermal parameters (conductivity and interface conductance) by using only the two hemispherical temperatures T^+ and T^- distinguishing the phonon populations according to the direction of their velocities have been proposed. It leads to a simple and comprehensive model able to accurately describe the heat transfer through heterostructures in all phonon transport regimes.

First, in homogeneous materials, we used the concept of effective conductivity which is relevant in all transport regimes. In ballistic regime, it becomes the ballistic conductance. These conductivities are related to a non-local temperature differences and are geometry dependent unlike the Fourier thermal conductivity. Second, the interface thermal conductance was defined by using the hemispherical temperatures. It appears to be an appealing solution

to make the interface thermal conductance modeling consistent with Monte Carlo simulation. When combining these three concepts, the historic virtual interface paradox is elegantly solved.

Finally, a comprehensive analytical framework has been derived using the central relationship between the heat flux and the local hemispherical temperature difference $Q = G_{\text{ballistic}}\,(T^{+} - T^{-})$ which allows us to do without the standard temperature. This framework extends the validity range of previous models while it only requires a set of three parameters: the effective conductivity $\kappa_{\text{effective}}$, the ballistic conductance $G_{\text{ballistic}}$ and the interface thermal conductance G^{I}. These parameters can be computed semi-analytically from the phonon dispersion, the phonon scattering rates and the geometry of the structure. The resulting model can accurately reproduce results of numerical Monte Carlo simulations in diffusive Si/Si junctions and Si/Ge heterostructures in all transport regimes, i.e. ballistic, diffusive, and intermediate ones.

This versatile and easy to use approach should be particularly suitable to investigate numerically or experimentally heat transfer in various kinds of complex nanostructures.

Acknowledgements

This work was supported by JST CREST Grant Number JPMJCR19Q3, Japan and a public grant overseen by the French National Research Agency (ANR) as part of the "Investissements d'Avenir" program (Labex NanoSaclay, reference: ANR-10-LABX-0035).

References

[1] J. B. J. baron Fourier, *Théorie Analytique de La Chaleur* (F. Didot, 1822).
[2] R. Peierls, *Zur Kinetischen Theorie Der Wärmeleitung in Kristallen*, Annalen Der Physik **395**, 1055 (1929).
[3] S. Narasimhan and D. Vanderbilt, *Anharmonic Self-Energies of Phonons in Silicon*, Physical Review B **43**, 4541 (1991).
[4] D. A. Broido, M. Malorny, G. Birner, N. Mingo, and D. A. Stewart, *Intrinsic Lattice Thermal Conductivity of Semiconductors from First Principles*, Appl. Phys. Lett. **91**, 231922 (2007).
[5] K. Esfarjani, G. Chen, and H. T. Stokes, *Heat Transport in Silicon from First-Principles Calculations*, Phys. Rev. B **84**, 085204 (2011).
[6] J. Shiomi, K. Esfarjani, and G. Chen, *Thermal Conductivity of Half-Heusler Compounds from First-Principles Calculations*, Phys. Rev. B **84**, 104302 (2011).
[7] G. Fugallo, M. Lazzeri, L. Paulatto, and F. Mauri, *Ab Initio Variational Approach for Evaluating Lattice Thermal Conductivity*, Physical Review B **88**, 045430 (2013).
[8] A. Seko, A. Togo, H. Hayashi, K. Tsuda, L. Chaput, and I. Tanaka, *Prediction of Low-Thermal-Conductivity Compounds with First-Principles Anharmonic Lattice-Dynamics Calculations and Bayesian Optimization*, Physical Review Letters **115**, 205901 (2015).
[9] D. G. Cahill, P. V. Braun, G. Chen, D. R. Clarke, S. Fan, K. E. Goodson, P. Keblinski, W. P. King, G. D. Mahan, A. Majumdar, H. J. Maris, S. R. Phillpot, E. Pop, and L. Shi, *Nanoscale Thermal Transport. II. 2003–2012*, Applied Physics Reviews **1**, 011305 (2014).
[10] T. Thu Trang Nghiêm, J. Saint-Martin, and P. Dollfus, *New Insights into Self-Heating in Double-Gate Transistors by Solving Boltzmann Transport Equations*, Journal of Applied Physics **116**, 074514 (2014).
[11] J. P. Heremans, M. S. Dresselhaus, L. E. Bell, and D. T. Morelli, *When Thermoelectrics Reached the Nanoscale*, Nature Nanotechnology **8**, 471 (2013).
[12] V. Hung Nguyen, M. C. Nguyen, H.-V. Nguyen, J. Saint-Martin, and P. Dollfus, *Enhanced Thermoelectric Figure of Merit in Vertical Graphene Junctions*, Applied Physics Letters **105**, 133105 (2014).
[13] P. Dollfus, V. H. Nguyen, and J. Saint-Martin, *Thermoelectric Effects in Graphene Nanostructures*, Journal of Physics: Condensed Matter **27**, 133204 (2015).
[14] Y. Chalopin, K. Esfarjani, A. Henry, S. Volz, and G. Chen, *Thermal Interface Conductance in Si/Ge Superlattices by Equilibrium Molecular Dynamics*, Physical Review B **85**, 195302 (2012).

[15] D. P. Sellan, E. S. Landry, J. E. Turney, A. J. H. McGaughey, and C. H. Amon, *Size Effects in Molecular Dynamics Thermal Conductivity Predictions*, Physical Review B **81**, 214305 (2010).
[16] S. Mazumder and A. Majumdar, *Monte Carlo Study of Phonon Transport in Solid Thin Films Including Dispersion and Polarization*, Journal of Heat Transfer **123**, 749 (2001).
[17] D. Lacroix, K. Joulain, and D. Lemonnier, *Monte Carlo Transient Phonon Transport in Silicon and Germanium at Nanoscales*, Physical Review B **72**, 064305 (2005).
[18] J.-P. M. Péraud, C. D. Landon, and N. G. Hadjiconstantinou, *Monte Carlo Methods for Solving the Boltzmann Transport Equation*, Annual Review of Heat Transfer **17**, 205 (2014).
[19] B. Davier, J. Larroque, P. Dollfus, L. Chaput, S. Volz, D. Lacroix, and J. Saint-Martin, *Heat Transfer in Rough Nanofilms and Nanowires Using Full Band* Ab Initio *Monte Carlo Simulation*, Journal of Physics: Condensed Matter **30**, 495902 (2018).
[20] F. Mazzamuto, V. Hung Nguyen, Y. Apertet, C. Caër, C. Chassat, J. Saint-Martin, and P. Dollfus, *Enhanced Thermoelectric Properties in Graphene Nanoribbons by Resonant Tunneling of Electrons*, Phys. Rev. B **83**, 235426 (2011).
[21] N. Mingo, L. Yang, D. Li, and A. Majumdar, *Predicting the Thermal Conductivity of Si and Ge Nanowires*, Nano Letters **3**, 1713 (2003).
[22] J. Ordonez-Miranda, R. Yang, and J. J. Alvarado-Gil, *A Constitutive Equation for Nano-to-Macro-Scale Heat Conduction Based on the Boltzmann Transport Equation*, Journal of Applied Physics **109**, 084319 (2011).
[23] A. A. Maznev, J. A. Johnson, and K. A. Nelson, *Onset of Nondiffusive Phonon Transport in Transient Thermal Grating Decay*, Phys. Rev. B **84**, 195206 (2011).
[24] C. Hua and A. J. Minnich, *Transport Regimes in Quasiballistic Heat Conduction*, Phys. Rev. B **89**, 094302 (2014).
[25] J.-P. M. Péraud and N. G. Hadjiconstantinou, *Extending the Range of Validity of Fourier's Law into the Kinetic Transport Regime via Asymptotic Solution of the Phonon Boltzmann Transport Equation*, Phys. Rev. B **93**, 045424 (2016).
[26] A. T. Ramu and J. E. Bowers, *A Generalized Enhanced Fourier Law*, Journal of Heat Transfer **139**, 034501 (2017).
[27] G. Chen, *Ballistic-Diffusive Heat-Conduction Equations*, Phys. Rev. Lett. **86**, 2297 (2001).
[28] K. T. Regner, A. J. H. McGaughey, and J. A. Malen, *Analytical Interpretation of Nondiffusive Phonon Transport in Thermoreflectance Thermal Conductivity Measurements*, Phys. Rev. B **90**, 064302 (2014).
[29] F. Yang and C. Dames, *Heating-Frequency-Dependent Thermal Conductivity: An Analytical Solution from Diffusive to Ballistic Regime and Its Relevance to Phonon Scattering Measurements*, Phys. Rev. B **91**, 165311 (2015).
[30] J. Maassen and M. Lundstrom, *Modeling Ballistic Effects in Frequency-Dependent Transient Thermal Transport Using Diffusion Equations*, Journal of Applied Physics **119**, 095102 (2016).
[31] P. Kapitza, *The Study of Heat Transfer in Helium II*, J. Phys.(USSR) **4**, 181 (1941).
[32] W. A. Little, *The transport of heat between dissimilar solids at low temperatures*, Can. J. Phys **37**, 334 (1959).
[33] E. T. Swartz and R. O. Pohl, *Thermal Boundary Resistance*, Reviews of Modern Physics **61**, 605 (1989).
[34] S. Simons, *On the Thermal Contact Resistance between Insulators*, J. Phys. C: Solid State Phys. **7**, 4048 (1974).
[35] G. Chen, *Thermal Conductivity and Ballistic-Phonon Transport in the Cross-Plane Direction of Superlattices*, Phys. Rev. B **57**, 14958 (1998).
[36] S. Merabia and K. Termentzidis, *Thermal Conductance at the Interface between Crystals Using Equilibrium and Nonequilibrium Molecular Dynamics*, Physical Review B **86**, (2012).
[37] T. Feng, W. Yao, Z. Wang, J. Shi, C. Li, B. Cao, and X. Ruan, *Spectral Analysis of Nonequilibrium Molecular Dynamics: Spectral Phonon Temperature and Local Nonequilibrium in Thin Films and across Interfaces*, Phys. Rev. B **95**, 195202 (2017).
[38] J. Maassen and V. Askarpour, *Phonon Transport across a Si–Ge Interface: The Role of Inelastic Bulk Scattering*, APL Materials **7**, 013203 (2019).

[39] X. Ran, Y. Guo, and M. Wang, *Interfacial Phonon Transport with Frequency-Dependent Transmissivity by Monte Carlo Simulation*, International Journal of Heat and Mass Transfer **123**, 616 (2018).
[40] J. Kaiser, T. Feng, J. Maassen, X. Wang, X. Ruan, and M. Lundstrom, *Thermal Transport at the Nanoscale: A Fourier's Law vs. Phonon Boltzmann Equation Study*, Journal of Applied Physics **121**, 044302 (2017).
[41] R. Kim, S. Datta, and M. S. Lundstrom, *Influence of Dimensionality on Thermoelectric Device Performance*, J. Appl. Phys. **105**, 034506 (2009).
[42] J. S. Martin, A. Bournel, and P. Dollfus, *On the Ballistic Transport in Nanometer-Scaled DG MOSFETs*, IEEE Transactions on Electron Devices **51**, 1148 (2004).
[43] C. Jeong, R. Kim, M. Luisier, S. Datta, and M. Lundstrom, *On Landauer versus Boltzmann and Full Band versus Effective Mass Evaluation of Thermoelectric Transport Coefficients*, J. Appl. Phys. **107**, 023707 (2010).
[44] R. Chen, A. I. Hochbaum, P. Murphy, J. Moore, P. Yang, and A. Majumdar, *Thermal Conductance of Thin Silicon Nanowires*, Physical Review Letters **101**, 105501 (2008).
[45] J. Maassen and M. Lundstrom, *Modeling Ballistic Effects in Frequency-Dependent Transient Thermal Transport Using Diffusion Equations*, Journal of Applied Physics **119**, 095102 (2016).
[46] Z. Liang, K. Sasikumar, and P. Keblinski, *Thermal Transport across a Substrate–Thin-Film Interface: Effects of Film Thickness and Surface Roughness*, Phys. Rev. Lett. **113**, 065901 (2014).
[47] J. Larroque, P. Dollfus, and J. Saint-Martin, *Phonon Transmission at Si/Ge and Polytypic Ge Interfaces Using Full-Band Mismatch Based Models*, Journal of Applied Physics **123**, 025702 (2018).
[48] L. N. D., D. B., D. P., and S.-M. J, *Study of Phonon Transport across Several Si/Ge Interfaces Using Full-Band Phonon Monte Carlo Simulation*, ArXiv:2102.10833 [Cond-Mat, Physics:Physics] (2021).